ResearchGate

See discussions, stats, and author profiles for this publication at: https://www.researchgate.net/publication/344040198

Predicting Tensile Properties of AZ31 Magnesium Alloys by Machine Learning

Article *in* JOM: the journal of the Minerals, Metals & Materials Society · September 2020

DOI: 10.1007/s11837-020-04343-w

CITATIONS
0

READS
56

4 authors, including:

Leyun Wang

38 PUBLICATIONS **855** CITATIONS

SEE PROFILE

Gaoming Zhu

Shanghai Jiao Tong University

21 PUBLICATIONS **94** CITATIONS

SEE PROFILE

Fanqi Meng

Hohai University

152 PUBLICATIONS **2,937** CITATIONS

SEE PROFILE

Some of the authors of this publication are also working on these related projects:

Deformation mechanism of magnesium alloy View project

Ductile Magnesium View project

All content following this page was uploaded by Gaoming Zhu on 05 October 2020.

The user has requested enhancement of the downloaded file.

JOM
https://doi.org/10.1007/s11837-020-04343-w
© 2020 The Minerals, Metals & Materials Society

Predicting Tensile Properties of AZ31 Magnesium Alloys by Machine Learning

XUENAN XU,[1,4] LEYUN WANG,[1,2,5] GAOMING ZHU,[1] and XIAOQIN ZENG[1,3]

1.—National Engineering Research Center of Light Alloy Net Forming, School of Materials Science and Engineering, Shanghai Jiao Tong University, Shanghai 200240, China. 2.—Materials Genome Initiative Center, Shanghai Jiao Tong University, Shanghai 200240, China. 3.—State Key Laboratory of Metal Matrix Composites, Shanghai Jiao Tong University, Shanghai 200240, China. 4.—School of Electronics, Information and Electrical Engineering, Shanghai Jiao Tong University, Shanghai 200240, China. 5.—e-mail: leyunwang@sjtu.edu.cn

AZ31 magnesium alloys from different suppliers usually have different chemistry and processing histories, causing variance in their mechanical properties. In this work, we establish the quantitative relationship between alloy compositions, processing parameters, and mechanical properties by machine learning. Based on the artificial neural network (ANN) and support vector machine (SVM) algorithms, two models were built using a dataset with 112 data. Both models achieved good accuracy in predicting yield strength (YS), ultimate tensile strength (UTS), and tensile elongation (EL). To test their generalization ability, a new AZ31 extruded alloy was fabricated, with its chemical composition and processing history being documented. The YS, UTS, and EL of this material were measured and compared with model predictions. Relative errors for YS, UTS, and EL were 5.4%, 23%, and 272% by the ANN model, and 28%, 25%, and 143% by the SVM model, respectively. The reasons for the overestimation of the mechanical properties are discussed.

INTRODUCTION

Magnesium (Mg) alloys possess low density, high specific strength, and good biocompatibility, making them attractive structural materials in the automotive, aerospace, and biomedical industries. The mechanical properties of Mg wrought alloys depend on the chemical composition and the processing history, which control the microstructure, such as grain size, texture, and precipitates.[1,2]

Mg wrought alloy development is typically conducted by trial and error. It relies on empirical experience and local optimization. Adjustable variables include the concentration of each alloying element (e.g., Al, Zn, Mn, Ca, Si, etc.) and the processing parameters (e.g., homogenization temperature and duration, rolling/extrusion temperature and speed, annealing temperature and duration, etc.). To find the optimal combination of variables, one has to fabricate different alloys and test each of them in a large searching space, which is a costly process.

Machine learning is a promising approach to accelerate the design of new Mg alloys. Machine learning has already made some well-known achievements in computer vision, natural language processing, speech recognition, and financial analysis. Recently, machine learning has been applied in materials science for new compound discovery,[3] physical properties prediction,[4,5] fatigue life and crack location prediction,[6,7] twin nucleation prediction,[8] steel and high entropy alloy design,[9,10] and automatic microstructure analysis.[11,12]

Artificial neural network (ANN) and support vector machine (SVM) are the most commonly used machine-learning algorithms in the materials science community. Using an SVM-based model, Shen et al.[9] investigated the influence of chemical composition (C%, Cr%, Ni%, Co%, Mo%, Ti%) and

(Received April 25, 2020; accepted August 19, 2020)

Published online: 01 September 2020

aging conditions on the hardness of martensitic stainless steels. The optimal model achieves $R^2 = 0.93$ for hardness prediction of the development set (i.e., the test set). While hardness is an important indicator of the yield strength (YS) of metallic materials, it does not directly relate to the ultimate tensile strength (UTS) and tensile elongation (EL), which are equally important metrics for structural materials' performance.

In the present paper, we employ ANN and SVM algorithms to build models for predicting the YS, UTS, and EL of AZ31, the most widely used commercial Mg wrought alloy. The dataset contains 112 data entries collected from the literature. Each data item is associated with an AZ31 alloy whose composition and processing history are described by 16 attribute values. Using this dataset, an ANN model and a SVM model were built independently to predict the YS, UTS, and EL from the 16 attribute values of an AZ31 alloy. To test the generalization ability of the models, a new AZ31 extruded alloy was fabricated by ourselves, with its chemical composition and processing history being documented. The YS, UTS, and EL values of this material were measured from a tensile test and then compared with the model predictions. The performance of the two models will be assessed.

METHODS

Data Collection

Data used for model training and testing have been collected from Refs. [13–23]. Initially, a much larger body of literature was searched, but data in many papers were incomplete (i.e., missing several key attribute values) and had to be dropped. On the other hand, if a data item only lacks one or two attribute values, it may be still usable. Specifically, the following rules were employed for data collection:

(1) If a data item misses only one or two attribute values, the mean value of these attributes from the whole dataset is used as an approximation. This is a common data pre-processing practice in machine learning.
(2) Data with missing output values (YS, UTS, or EL) are excluded.
(3) Only rolled or extruded alloys are included in the dataset. For rolled alloys, the attributes associated with extrusion (e.g., extrusion temperature, extrusion ratio) are set as zero, and vice versa. Alloys fabricated by exotic processing methods such as equal channel angular processing or high-pressure torsion have been excluded.
(4) Homogenization and annealing are optional processing steps before or after extrusion/rolling. If a data item does not involve those optional steps, the corresponding attributes (homogenization temperature and duration, annealing temperature and duration) take values of zero. This practice is reasonable since the attribute with a zero value will not influence the activation value of the next layer whatever the weights.

Based on the above rules, a total of 112 useful data were eventually collected.

Machine Learning Algorithms and Model Training

Artificial Neural Network (ANN)

ANN is one of the most popular algorithms in modern machine learning.[24] The algorithm combines linear transformation and non-linear activation functions to simulate complex nonlinear systems. A basic ANN consists of three interconnected layers: an input layer, a hidden layer, and an output layer. The input layer is a vector of the attribute values of a data item. The hidden layer consists of certain number of "neurons", whose values are computed by linear transformation of the input vector. The weights and bias for the linear transformation of each hidden neuron are to be determined. By further applying a nonlinear activation function like sigmoid or ReLU (i.e., rectified linear unit), the values of each neuron in the hidden layer are obtained. A similar process (i.e., linear transformation + nonlinear activation) is taken to compute the output layer from the hidden layer.

Training of the neural network (i.e., determining the weights and bias for the linear transformations) is realized by standard back propagation: the weights and bias are initially set as random values and updated in each training epoch to minimize the difference between the predicted outputs and their actual values over all data from the training set (i.e., system loss). This is known as the "gradient descent" approach. More details about the ANN algorithm can be found in Ref. 24.

In the present work, a fully-connected neural network was built, which contained an input layer, a hidden layer with 50 neurons, and an output layer. The input layer was a vector of 16 attributes describing the chemical composition and processing parameters of each data item, as shown in Table I. The output layer contains three outputs: YS, UTS, and EL. The ReLU activation function was used. The neural network was built and trained in the *PyTorch* framework in Python.[25] He initialization[26] was used for the initialization of the weights and bias. The model was trained using the Adam optimization strategy, which adopts an adaptive learning rate. The initial learning rate was set as 5×10^{-4}. A graphic illustration of the model is shown in Fig. 1.

Table I. The definitions and ranges of different attributes for the 112 data

Composition of Zn (%)	0.28–1.01
Composition of Al (%)	0.39–3.28
Composition of Mn (%)	0–1.06
Composition of Ca (%)	0–0.05
Composition of Si (%)	0–0.26
Homogenization temperature (°C)	360–418
Homogenization duration (h)	4–72
Extrusion temperature (°C)	20–400
Extrusion ratio	4–166
Extrusion speed (mm/s)	1–17
Rolling temperature (°C)	200–400
Rolling reduction (%)	20–86
Rolling speed (mm/s)	33–500
Annealing temperature (°C)	150–500
Annealing duration (h)	0.5–96
Angle between loading and processing direction (°)	0/45/90
Yield strength (MPa)	85–280
Ultimate tensile strength (MPa)	178–350
Elongation (%)	4–39

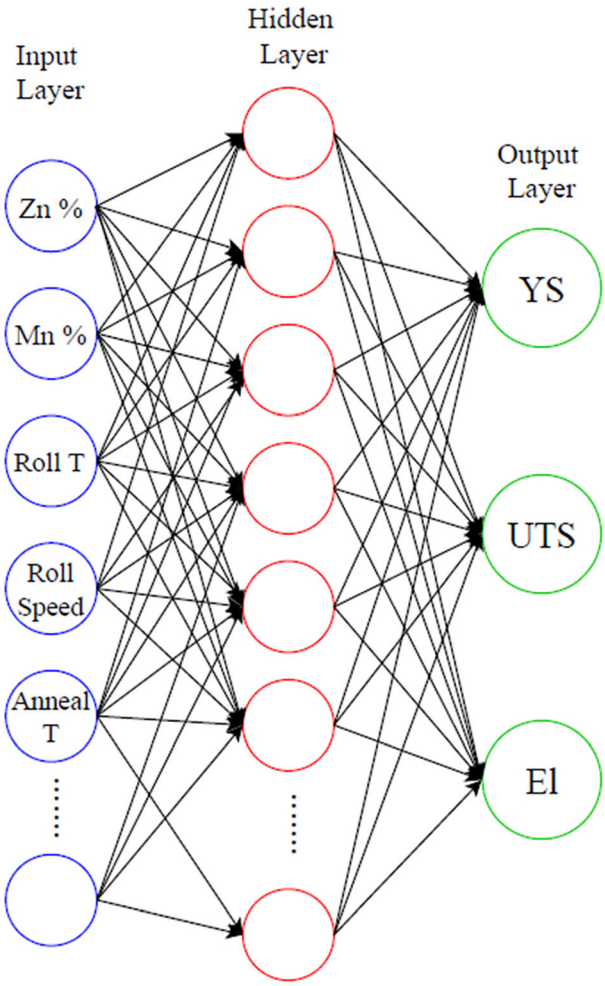

Fig. 1. The ANN model.

Support Vector Machine (SVM)

SVM is another popular algorithm widely used for classification and regression analysis. Any dataset can be viewed as points in a high-dimensional space. For binary classification tasks, an SVM classifier aims to draw a decision boundary, which not only separates the data of the two classes but also stays as far from the closest instances (i.e., support vectors) in each class as possible. One can think of an SVM classifier as fitting the widest possible street between the classes. An SVM regression model is similar to an SVM classification model while reversing the objective: instead of trying to fit the largest possible street between two classes, SVM regression tries to fit as many instances as possible on the street while limiting margin violations (i.e., instances off the street). The regression function can be linear or nonlinear. To tackle nonlinear regression tasks, the so-called "kernel trick" is adopted to project input data to a higher-dimensional space. SVM is very suitable for training a regression model using a small-size dataset because only those support vectors matter for the model.

In the present work, the SVM model was built and trained using the *sklearn* package in Python.[27] The radial basis function kernel was used. There are two hyper-parameters in the model: C and γ. C is a penalty coefficient that controls the generalization ability of the model; γ dictates the number of support vectors. In this model, C is set as 50, and γ takes the default value in *sklearn* (i.e., inverse of the number of attributes = 1/16).

Model Training

For the training of the ANN model, the whole dataset was split into a training set and a development set, with the training set further split into a

training subset and a validation subset. The proportions between the training subset, the validation subset, and the development set were 60%:20%:20%. In each training iteration, the ANN model was trained for 2000 epochs. There were three training iterations on the training subset, and each iteration generated a model. The model that yielded the lowest loss on the validation subset was selected.

It is worth mentioning that the definition of the loss is modified in our model. For a model that generates multiple outputs, the loss value is conventionally defined as the sum of the $L1$ loss for all outputs, where the $L1$ loss is the sum of the absolute difference between the ground true and the predicted value over all the training data. However, because the prediction of EL is often more difficult than the prediction of YS and UTS, the $L1$ loss on the EL output is penalized 10 times more than the $L1$ loss on the other two outputs. Therefore, the loss function is defined as follows:

$$\ell = \ell(\mathrm{YS}) + \ell(\mathrm{UTS}) + 10 * \ell(\mathrm{El}) \qquad (1)$$

where $\ell(x)$ means standard $L1$ loss on output x.

For the training of the SVM model, three independent models were built to target the three outputs (YS, UTS, and EL) separately. Like the training of the ANN model, several SVM models with different hyper-parameters were trained using the same training subset. The validation subset was again used to pick the best model.

DATASET EXPLORATION

The dataset for the model training and testing is briefly described here. Among the 112 data, 76 were rolled alloys and the other 36 were extruded alloys. The ranges of different attributes and mechanical properties are listed in Table I.

Figure 2 shows the distribution histogram of the YS, UTS, and EL from the dataset. The YS values of the 112 data approximately follow a Gaussian distribution with the mean value around 160 MPa. The UTS and EL values are more scattered, since they are more sensitive to the microstructure and defects in the material.

To assess how individual attributes affect the YS, UTS, and EL, the Pearson correlation coefficients have been calculated and are plotted by a heat map in Fig. 3. Darker squares denote higher correlation coefficients between the attribute and the output. From this figure, some qualitative conclusions can be drawn. For example, the concentrations of Zn and Al have a stronger effect on the material's UTS and EL than on its YS. EL is also very sensitive to the concentration of Ca.

The dataset contains both extruded alloys and rolled alloys. When calculating the correlation coefficient between the extrusion/rolling parameters and outputs, only the extruded/rolled alloys have been used.

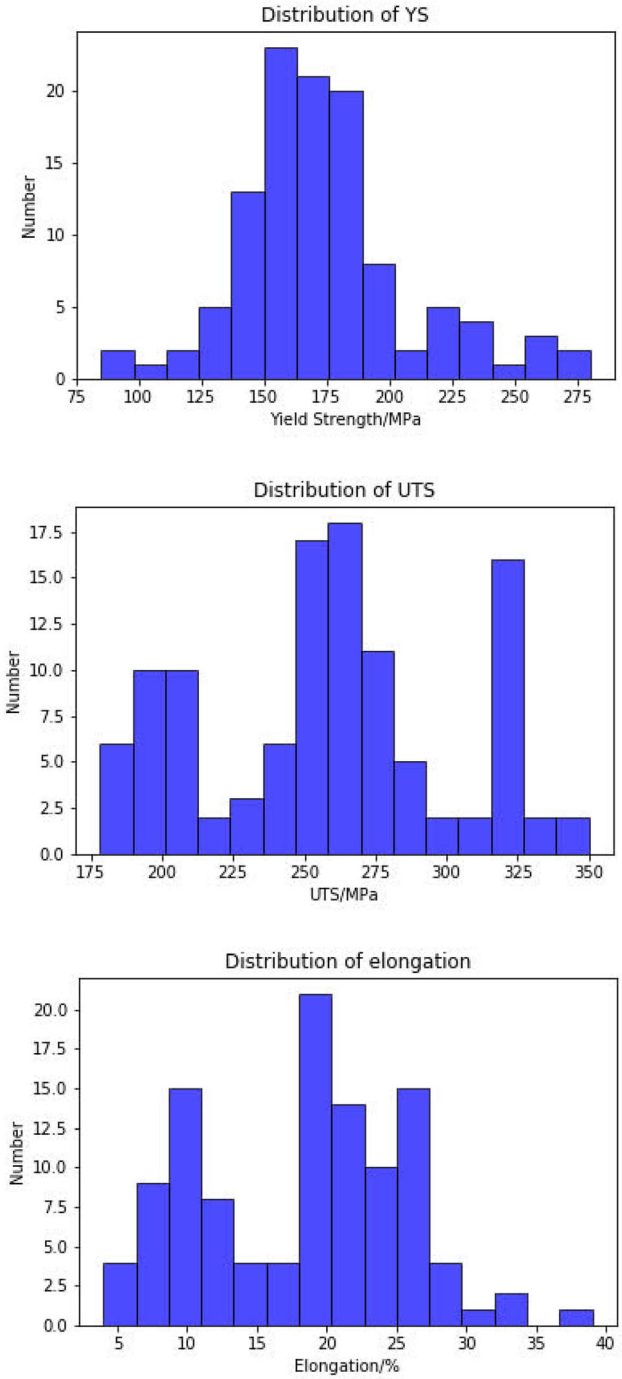

Fig. 2. Distribution of YS, UTS, and EL from the dataset.

MODELING RESULTS

The ANN Model

The training of the ANN model is demonstrated in Fig. 4, which plots the evolution of the loss value on the training, validation, and development sets. The loss decreased rapidly at the beginning; after 2000 epochs, loss on the training, validation, and development sets became stabilized. A clear gap between the training loss and the validation/development

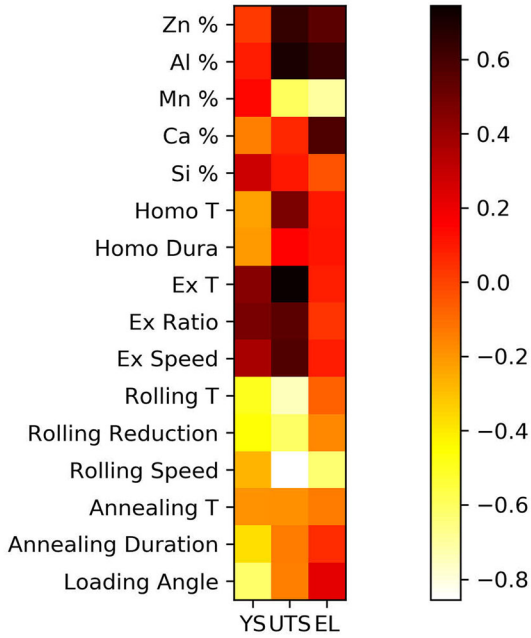

Fig. 3. Correlation coefficients between attributes and outputs.

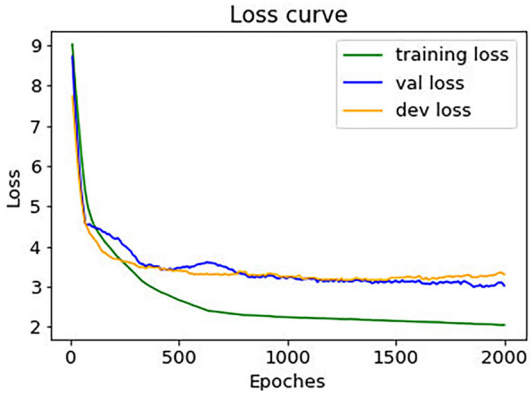

Fig. 4. The loss curves on different subsets during training.

loss can be observed, suggesting that there is certain level of overfitting. This is mainly due to the small size of the dataset.

The trained model was applied on the development set to test the quality of the model. The comparison between the predicted outputs (YS, UTS, EL) and the ground true values in the development set are shown in Fig. 5(a). The R^2 values (coefficient of determination) for YS, UTS, and EL prediction are 0.83, 0.83, and 0.86, respectively. The near-equal R^2 values for the three outputs justify the usage of the loss function in Eq. 1.

The SVM Model

Similar comparisons between the predicted output values by the SVM model versus ground true values are shown in Fig. 5b. The R^2 values for the YS, UTS, and EL predictions are 0.79, 0.93, and 0.79, respectively. For the YS and UTS predictions, the fitted lines almost coincide with the $y = x$ line, which indicates that the prediction values are very close to the ground true values. For the EL prediction, the fitted line of predicted elongation versus ground true elongation is above the $y = x$ line, which indicates that the model slightly overestimates the material's elongation.

Model Assessment Using New Experimental Data

While the development set allows us to assess the two models' performance, there is still a drawback: division of the original dataset was random, so some data in the development set and other data in the training set may come from the same literature, which may artificially boost the performance of the model. A more rigorous way to assess the model performance is fabricating a new AZ31 alloy and then measuring its YS, UTS, and EL values via a tensile test. Thus, we fabricated an AZ31 extruded alloy. Its chemical composition and processing parameters are shown in Table II. A dog-bone tensile specimen with gauge dimension of 11.0 mm (L) × 4.0 mm (W) × 1.4 mm (T) was extracted from the extrusion bar and tested using a MICROTEST 200 N (Deben, UK) module. The tensile direction is parallel with the extrusion direction. More details of the experiment can be found in Ref. 28. From this test, the YS, UTS, and EL values of this material were obtained.

From the inputs in Table II, we used the ANN model and the SVM model to predict the YS, UTS, and EL values and Table III compares the measured and predicted values. Both models overestimated the YS, UTS, and EL values. Using the ANN model, relative errors for YS, UTS, and EL are 5.4%, 23%, and 272%; using the SVM model, relative errors for YS, UTS, and EL are 28%, 25%, and 143%, respectively. While the prediction errors for YS and UTS are acceptable, both models largely overestimate the elongation. The reasons will be discussed in the next section.

DISCUSSION

Both the ANN and the SVM models achieved good prediction for the development set, while neither of them successfully predicted the mechanical properties of an AZ31 alloy fabricated and tested by ourselves. There are a few possible explanations. First, the training set is relatively small because only a tiny fraction of the literature provided full details of the material's chemical composition and processing parameters. This heightens the urgency to establish a standard for material data reporting in the academic publishing business. Second, published data tend to be "good data". YS, UTS, and EL values from these papers are most likely higher than the average values. Many "bad data" are

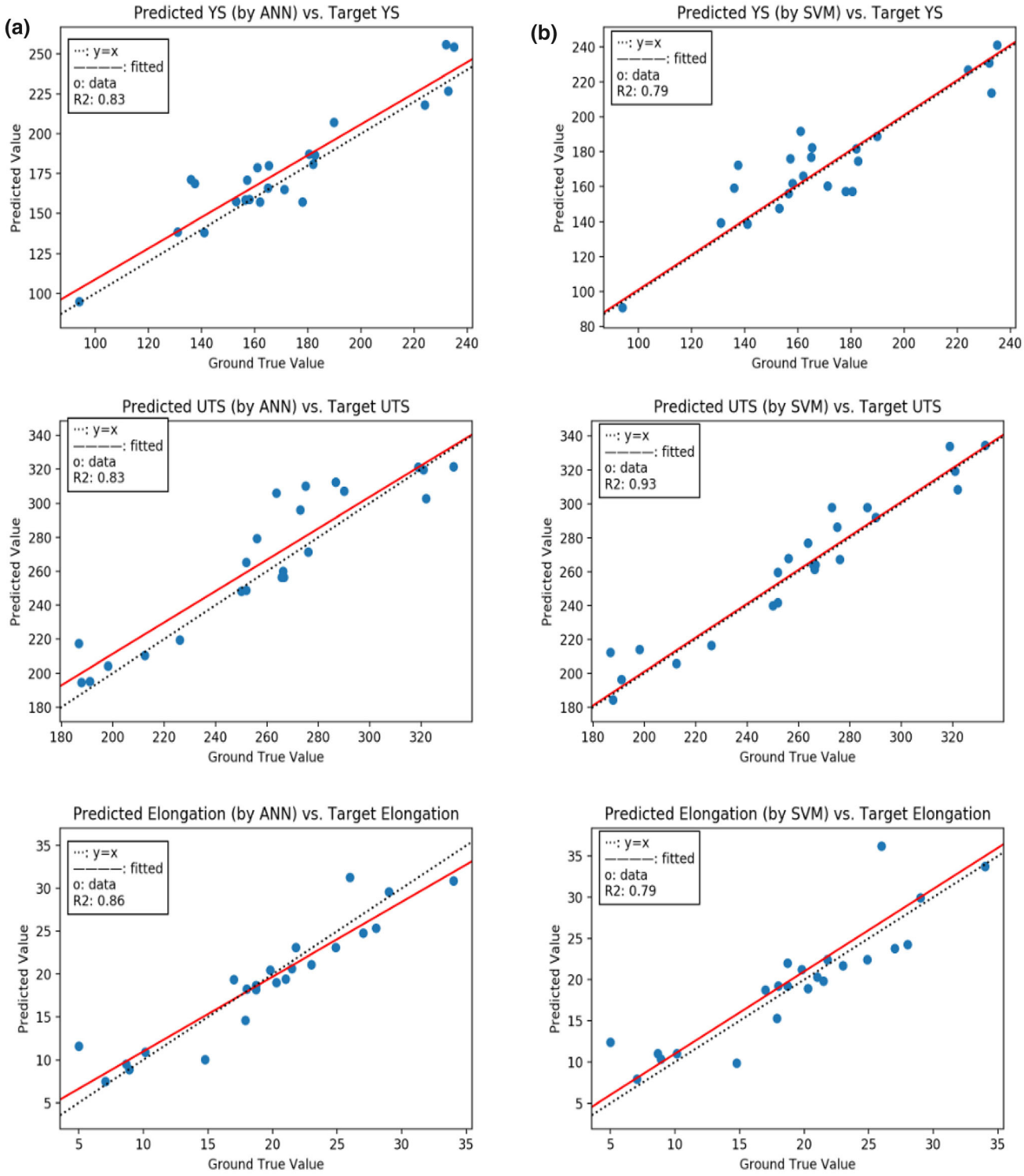

Fig. 5. Comparison of the predicted YS, UTS, and EL values using (a) the ANN model and (b) the SVM model with the ground true values from the development set.

unfortunately discarded and never shown in the literature. This practice inevitably leads to bias when we only use "good data" to build machine-learning models. Future efforts should be made to recycle those "bad data", which are equally valuable for machine-learning-based modeling as "good data". Third, the texture effect may be underestimated in our current model setting. While the angle between the loading direction and the extrusion/rolling directions is used as an input attribute, perhaps it has not sufficiently emphasized the texture effect. When the tensile loading is parallel

Table II. Composition and processing parameters of a new AZ31 alloy

Composition of Zn (%)	0.7489
Composition of Al (%)	2.998
Homogenization temperature (°C)	400
Homogenization duration (h)	24
Extrusion temperature (°C)	350
Extrusion ratio	18
Extrusion speed (mm/s)	2
Angle between loading and processing direction (°)	0
Annealing temperature (°C)	500
Annealing duration (h)	1

Table III. Measured and predicted values of YS, UTS, and EL of the AZ31 alloy

	YS (MPa)	UTS (MPa)	Elongation (%)
Measured	148	208	7
ANN prediction	156	256	26
SVM prediction	189	259	17

to the extrusion direction, most of the grains will have a near-zero Schmid factor for the easiest basal slip and a negative Schmid factor for twin nucleation.[29,30] As a result, such alloys will have low elongation due to the lack of deformation systems. In contrast, when the tensile loading is 45° or 90° from the extrusion direction, basal slip and twinning can be much more easily activated, which usually leads to higher elongation. This may explain why the two models dramatically overestimate the elongation value in Table III. It further implies that microstructure information and physical metallurgy knowledge should be considered in machine-learning models. Of course, that would impose even higher requirements for data collection.

CONCLUSION

In this paper, machine-learning-based models were built to predict the mechanical properties of AZ31 alloys from their composition and processing history. A dataset containing 112 data was compiled from the published literature. This dataset was divided into training, validation, and development sets in a ratio of 60%:20%:20%. An ANN model and a SVM model were developed from the training and validation sets. Both models achieved good prediction results for the development set. On the other hand, when the models were applied on a new extruded AZ31 alloy fabricated and tested by ourselves, all the properties were overestimated, especially the elongation. Possible reasons for this overestimation are discussed.

ACKNOWLEDGEMENTS

This work is financially supported by a collaborative research project (No. 18X120010001) between the University of Michigan and Shanghai Jiao Tong University which applies data science to Mg alloy design. We also acknowledge support from the National Key Research and Development Program of China (No. 2016YFB0701203) and the Science and Technology Commission of Shanghai Municipality (No. 18511109302).

CONFLICT OF INTEREST

The authors declare that they have no conflict of interest.

REFERENCES

1. S. Begum, D.L. Chen, S. Xu, and A.A. Luo, *Mater. Sci. Eng. A* 517, 334 (2009).
2. H. Pan, Y. Ren, H. Fu, H. Zhao, L. Wang, X. Meng, and G. Qin, *J. Alloys Compd.* 663, 321 (2016).
3. P. Raccuglia, K. Elbert, P. Adler, C. Falk, M. Wenny, A. Mollo, M. Zeller, S. Friedler, J. Schrier, and A. Norquist, *Nature* 533, 73 (2016).
4. R. Ramprasad, R. Batra, G. Pilania, A. Mannodi-Kanakkithodi, and C. Kim, *npj Comput. Mater.* 3, 54 (2017).
5. Y. Zhang and C. Ling, *npj Comput. Mater.* 4, 25 (2018).
6. A. Agrawal and A. Choudhary, *APL Mater.* 4, 053208 (2016).
7. A. Rovinelli, M. Sangid, H. Proudhon, and W. Ludwig, *Npj Comput. Mater.* 4, 35 (2018).
8. Z. Tong, L. Wang, G. Zhu, and X. Zeng, *Metall. Mater. Trans. A* 50A, 5543 (2019).
9. C. Shen, C. Wang, X. Wei, Y. Li, S.V.D. Zwaag, and W. Xu, *Acta Mater.* 179, 201 (2019).
10. C. Wen, Y. Zhang, C. Wang, D. Xue, Y. Bai, S. Antonov, L. Dai, T. Lookman, and Y. Su, *Acta Mater.* 170, 109 (2019).
11. B. DeCost, T. Francis, and E. Holm, *Acta Mater.* 133, 30 (2017).
12. Z. Chen and S. Daly, *Mater. Sci. Eng. A* 736, 61 (2018).
13. Y. Wang and H. Choo, *Acta Mater.* 81, 83 (2014).
14. Y. Chino, M. Mamoru, R. Kishihara, H. Hosokawa, Y. Yamada, C. Wen, K. Shimojima, and H. Iwasaki, *Mater. Trans.* 43, 2254 (2002).
15. Y. Wang, C. Chang, C. Lee, H.K. Lin, and J.C. Huang, *Scr. Mater.* 55, 637 (2006).
16. S. Liang, Z. Liu, and E. Wang, *Rare Met. Mater. Eng.* 46, 1411 (2017).
17. A. Yamashita, Z. Horita, and T. Langdon, *Mater. Sci. Eng. A* 300, 142 (2001).

18. S. Liang, X. Wang, and Z. Liu, *Rare Met. Mater. Eng.* 38, 1276 (2009).
19. H. Luo, *Mater. Mech. Eng.* 37, 60 (2013).
20. L. Shi, J. Li, and Y. Li, *Forg. Stamp. Technol.* 34, 35 (2009).
21. P. Wu and X. Dai, *Hot Work. Technol.* 46, 136 (2017).
22. C. Zhao, G. Wang, and Y. Huang, *Hot Work. Technol.* 44, 231 (2015).
23. H. Lu. *Master Thesis*. Taiyuan University of Science and Technology (2017).
24. P. Tan, M. Steinbach, and V. Kumar, *Introduction to Data Mining* (New York: Pearson, 2005).
25. https://pytorch.org/tutorials/beginner/blitz/autograd_tutorial.html.
26. K. He, X. Zhang, S. Ren, and J. Sun, Proceedings of the IEEE international conference on computer vision, 1026 (2015).
27. A. Géron, *Hands-On Machine Learning with Scikit-Learn, Keras, and TensorFlow: Concepts, Tools, and Techniques to Build Intelligent Systems* (Sebastopol, CA: O'Reilly Media, 2019).
28. G. Zhu, L. Wang, H. Zhou, J. Wang, Y. Shen, P. Tu, H. Zhu, W. Liu, P. Jin, and X. Zeng, *Int. J. Plasticity* 120, 164 (2019).
29. H. Yu, C. Li, Y. Xin, A. Chapuis, X. Huang, and Q. Liu, *Acta Mater.* 128, 313 (2017).
30. Z.R. Zeng, Y.M. Zhu, R.L. Liu, S.W. Xu, C.H.J. Davies, J.F. Nie, and N. Birbilis, *Acta Mater.* 160, 97 (2018).

Publisher's Note Springer Nature remains neutral with regard to jurisdictional claims in published maps and institutional affiliations.

View publication stats